Journal of Anatomy

J. Anat. (2009) **214**, pp937–955 doi: 10.1111/j.1469-7580.2009.01075.x

Configuration of the setal fields of *Rhoptropus* (Gekkota: Gekkonidae): functional, evolutionary, ecological and phylogenetic implications of observed pattern

Megan K. Johnson and Anthony P. Russell

University of Calgary, Department of Biological Sciences, Calgary, Canada

Summary

Many gekkotans possess seta-bearing adhesive subdigital pads. Details of setal structure, however, are largely based upon putatively exemplary fibrils deemed typical of the species. Little is known of the pattern of configuration of the setae across the subdigital pads and how great, if any, the variance in structure and dimensions is. To understand setal fields as functional entities, as opposed to individual setae, it is necessary to consider this pattern. Additionally, gekkotans within individual radiations occupy different environments and potentially are substrate-specific in terms of the locomotor surface exploited. To investigate these issues, we herein examine the configuration and dimensions of seven species of the gekkotan genus *Rhoptropus*, and an outgroup taxon, *Chondrodactylus bibronii*. All of these taxa are rupicolous and the array of rock surfaces exploited by this cluster of taxa is extensive. Our results show that setal field configuration follows a predictable pattern, both from one digit to another within a species, and between homologous digits and anatomical locations between species. One species, *Rhoptropus afer*, a more terrestrial taxon, exhibits significantly shorter setae and a smaller subdigital pad area than do its congeners, but exhibits the same overall pattern of setal arrangement. Our findings have implications for the understanding of the evolution of adhesive structures, and for the principles used for generating and manufacturing biomimetic artificial microfibrillar arrays.

Key words adhesion; *Chondrodactylus*; Gekkota; locomotion; *Rhoptropus*; setae.

Introduction

The subdigital pads of gekkotans interact with locomotor surfaces via fields of setae composed of microfibrillar keratinous arrays carried on highly modified subdigital scales (Russell, 2002). The mode of action of the setae has been the focus of inquiry for well over a century, with successive hypotheses about the means of bonding with surfaces being advanced (Simmermacher, 1884; Tornier, 1899; Gadow, 1901; Weitlaner, 1902; Kunitzky, 1903; Tandler, 1903; Schmidt, 1905; Hora, 1923; Dellit, 1934, 1949; Mahendra, 1941; Altevogt, 1954; Maderson, 1964; Hiller, 1968, 1969, 1976; Autumn et al. 2000, 2002, 2006a; Huber et al. 2005; Sun et al. 2005; Tian et al. 2006). In recent years technological advances have enabled setae and setal arrays to be isolated and subjected to investigative techniques that have revealed a complex interaction of van der Waals and shear forces that permit the establishment, and breaking, of an adhesive bond (Autumn et al. 2000, 2006a; Tian et al. 2006).

In parallel with such investigations have been studies that have revealed that the dimensions of setae, and their pattern of arrangement, are highly variable across species (Ruibal & Ernst, 1965; Russell, 1976; Schleich & Kästle, 1986), and even along the digits within species (of both geckos and anoles) (Ruibal & Ernst, 1965; Peterson, 1983; Delannoy, 2006). Series of epidermal outgrowths from simple spines, to spikes, to prongs and ultimately fully developed setae are expressed along digits (Peterson & Williams, 1981; Peterson, 1983; Delannoy, 2006). Such morphological series are thought to reflect the evolutionary transition from simple outgrowths to the highly modified fibrils most readily associated with the adhesive process (Russell, 1976; Peterson, 1983).

Lengths of setae have been reported for a wide array of taxa (Ruibal & Ernst, 1965; Russell, 1972; Schleich & Kästle, 1986) and have generally been taken to be species-specific (Maderson, 1970; Autumn et al. 2000). Basic data about setal dimensions and packing density have been employed in the generation of synthetic microfibrillar arrays that simulate the adhesive capabilities of geckos (Geim et al.

Correspondence
Anthony P. Russell, University of Calgary, Department of Biological Sciences, 2500 University Drive NW, Calgary, AB T2N 1N4, Canada.
E: arussell@ucalgary.ca

Accepted for publication *19 February 2009*

2003; Sitti & Fearing. 2003; Hui et al. 2004; Kim et al. 2007; Kustandi et al. 2007; Lee et al. 2008). Such arrays are generally constructed of microfibrils of a single length that ostensibly mimic the structure of gekkotan setal fields. Such extrapolations beg the question of how well such approaches reflect the actual pattern of the configuration of gekkotan setal fields and, indeed, whether this actually matters.

Our objective herein, therefore, is to investigate the pattern of and potential assembly rules of gekkotan setal fields by conducting a comparative study of these characteristics in a single radiation for which information about locomotor substrate is known. In another publication we detail the attributes of species-specific substrate affinities. Herein we focus on the structure of the setal fields themselves, and place them into the context of the structure of the digits as the carrier and operator of the setal batteries (Russell, 1975), attempting to account for the configuration of the entire adhesive apparatus that is likely to influence the architecture of the setal fields as mechanical intermediaries between the organism and its locomotor environment (Russell et al. 2007).

It has long been recognized that closely related gekkotan taxa (such as members of a single genus) vary, among other things, in features of the configuration of their subdigital pads, such as the number of scansors/lamellae present on their digits and the relative dimensions of the pads. Such variation has been employed for taxonomic and systematic purposes, and has been assumed to be of evolutionary and ecological significance (Hecht, 1952; Collette, 1961). Within a single radiation, in which the basic pattern of the subdigital pads is homologous (Russell, 1976), we investigate the following hypotheses: setal dimensions will vary predictably according to station on the digit and on a given scansor; setal dimensions will vary in association with identifiable aspects of digital morphology; within a radiation there will be common assembly rules for the setal fields, with variation being related to subdigital pad dimensions and numbers of scansors and (to be explored elsewhere) with characteristics of the substrate exploited.

Materials and methods

Taxon selection

Selection of an example genus for investigating setal field morphology requires the fulfilment of a number of criteria. *Gekko gecko* (Linnaeus 1758) (the Tokay gecko) has served as a model organism for the majority of previous studies of the gekkotan adhesive system and adhesive performance. It has been employed largely because it is readily available and easy to maintain and house in captivity (Russell, 1976). Furthermore, the species is large by gecko standards (SVL = 15 cm, mass = 45 g) (Russell & Bauer, 1986; Delannoy, 2006) and has large, well-defined subdigital pads that are amenable to investigation of setal characteristics and the configuration of the adhesive system (Delannoy, 2006). The genus *Gekko,* however, is not well suited as an initial candidate for our purposes because it is very speciose, most species are not easily obtained or observable in the field, and little is known of the natural history of most species (Brown & Alcala, 1978, 2000; Brown et al. 2000; Roesler et al. 2006).

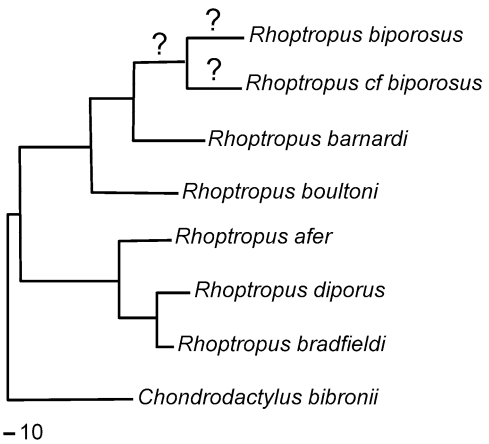

Fig. 1 Maximum parsimony tree for the genus *Rhoptropus*, with *Rhoptropus* cf. *biporosus* added at its most likely position (A. M. Bauer and T. Lamb, unpublished). Question marks indicate unknown branch lengths for the new species. A scale bar representing 10 base pair changes is shown.

The genus *Rhoptropus* (Fig. 1) from Namibia and Angola was selected as the taxon of focus for several reasons. It is diurnal, rupicolous and essentially clawless (Bauer & Good, 1996). It is part of the *Pachydactylus* lineage (Bauer & Good, 1996; Johnson et al. 2005). Members of *Rhoptropus* are restricted to arid and hyper-arid areas, occupy rocky outcrops and boulders, and run rapidly, jump and move with apparent ease across rock surfaces of all orientations. The array of eight species, *Rhoptropus afer* Peters 1869*, Rhoptropus barnardi* Hewitt 1926*, Rhoptropus biporosus* Fitzsimons 1957*, Rhoptropus boultoni* Schmidt 1933*, Rhoptropus bradfieldi* Hewitt 1935*, R. diporus* Haacke 1965*, R. taeniostictus* Laurent 1964, and one as yet undescribed species, exploit different locomotor substrata across a relatively small geographic range, enabling effective sampling and the investigation of intra- and interspecific variation in adhesive system morphology and associated substrate characteristics (to be reported elsewhere). *Rhoptropus taeniostictus* is found exclusively in Angola, and could not be included in the current study.

Members of *Rhoptropus* are medium-sized (SVL = 3.5–6.5 cm, mass = 1–6 g) geckos (Branch, 1988) and their phylogenetic relationships are well resolved (Fig. 1) (Bauer & Good, 1996; Lamb & Bauer, 2000, 2001, 2002; Bauer & Lamb, 2002, 2005). Like other *Pachydactylus* group taxa they are characterized by substrate-specific habitat preferences (Branch, 1988; Bauer & Good, 1996; Bauer & Lamb, 2005). Setal variation within and between species of *Rhoptropus* is contextualized by making comparisons with an outgroup species from the remainder of the *Pachydactylus* radiation, and with other gecko species that lie outside the *Pachydactylus* radiation.

Sampling and measurements

Specimens of seven species of *Rhoptropus* (*R. afer* – 3 specimens*, R. barnardi* – 3 specimens*, R. biporosus* – 4 specimens*, R. boultoni*

– 4 specimens, *R. bradfieldi* – 4 specimens, *R. diporus* – 3 specimens and a new, undescribed species that is the sister taxon to *R. biporosus* – A. M. Bauer, personal communication – henceforth referred to as *R.* cf. *biporosus* – 5 specimens), as well as the outgroup species *Chondrodactylus bibronii* (Smith, 1846) (21 specimens), were collected from various sites in Namibia in June and July 2005, under the auspices of a permit issued to Dr. Aaron M. Bauer. This provided a total sample size of 47 specimens (26 *Rhoptropus*), with each species being represented by at least three individuals. General attributes of the various species (except the newly discovered species) were established for much larger series (see Bauer et al. 1996 for a list of specimens), but invasive sampling was only permissible for smaller numbers. The extensive sampling of the series of *C. bibronii* (21 specimens) (Webster et al. 2009) permitted comparisons with the smaller *Rhoptropus* series and allowed identification of any patterns that were seemingly aberrant (no such aberrations were encountered). Pattern analysis was further anchored by comparison with the extensive series of *G. gecko* examined by Delannoy (2006) that again provided information about general principles of setal field patterning. The specimens of *Rhoptropus* examined now reside in the collections of the Museum of Comparative Zoology (MCZ), Harvard University, and the National Museum of Namibia (NMNW), Windhoek (see Table S1 in the Supporting Information for details).

The alcoholic museum specimens were weighed and their snout–vent lengths (SVL) measured. *Rhoptropus* and *Pachydactylus* are not sexually dimorphic and thus data for all specimens were pooled. One digit was removed from each specimen of *Rhoptropus* for detailed examination. For most species this was digit IV of the left pes; however, for *R. biporosus* and *R.* cf. *biporosus,* a variety of digits were removed to permit assessment of variation across the digits. For the outgroup species, *Chodrodactylus bibronii*, a sample of digits for 21 individuals were removed for examination (Webster et al. 2009). Details of specimen numbers, locality information and digits removed for examination are documented in Table S1 of the Supporting Information.

Following removal, digits were photographed using a Nikon DS-L1 digital camera mounted on a Nikon SMZ300 dissecting microscope, and operated via a Nikon DS-5M camera control unit. Measurements of pad area were taken from the images using the computer software ImageTool V.3.0. Measurements were taken for all expanded subdigital scales that appeared to bear setae or seta-like structures. These measurements were later calibrated to match the scansor (Russell, 1986) count obtained from scanning electron microscope (SEM) images of the same digit. Only scansors (Russell, 1986) (and not the more proximal lamellae) were included in the estimate of pad area for three reasons: first, the preparation of digits for SEM viewing generally resulted in the detachment of the outer epidermal (Oberhäutchen) layer from all subdigital scales except the scansors (where the layer is very tightly attached to the underlying epidermal layers and the dermis; Russell, 1986); secondly, because the pad area associated with the scansors alone (and not the more basal region of the digit) is more highly correlated with measurements of body size (Webster et al. 2009); and thirdly because subcutaneous control systems (Russell, 2002) are physically linked to the scansors but not to the lamellae. Therefore, concentrating on the scansors alone permits better control of cross-species comparisons.

Digits were subsequently prepared for SEM examination. Each was sagittally sectioned, and both halves of each digit were sequentially critical point dried using a Seevac CO_2 Critical Point Dryer; mounted on $^1/_2$-inch Zeiss aluminum flat endpin SEM mounts (Electron Microscopy Sciences, Hatfield, PA, USA) using colloidal silver paste, with one half mounted with the ventral side of the digit facing upward and the other half mounted on its side with the cut sagittal edge facing upward to reveal setal arrangement along the scansors; sputter coated with a 100-Å layer of gold particles in a Hummer II Sputter Coater; and viewed in the standard high vacuum mode of a Philips/FEI XL30 Environmental Scanning Electron Microscope (ESEM). Images were taken of entire digit halves, and also of each scansor, in both ventral and sagittal views. These images were stretched using the XL30 Stretch program to obtain images of correct proportions for measurement. Images were inputted into ImageTool V.3.0, and a variety of setal field measurements taken (Fig. 2).

A scansor count was determined and digit depth was also measured. Measurements of setal length were taken for all scansors of one specimen of each species to obtain a continuous representation of setal variation along the entire digital pad, and then for three representative scansors for all other specimens. These representative scansors are the distalmost scansor, an intermediate scansor (a middle scansor selected at the midpoint of the total number of scansors), and the proximalmost scansor. This allowed for comparison of functionally comparable scansors regardless of the total number of scansors present (Fig. 2).

Measurements recorded for each scansor examined were: scansor length, number of setal rows, maximum setal length, minimum setal length, mean setal length, maximum setal diameter, minimum setal diameter, mean setal diameter and setal resting angle (Fig. 2). Scansor length was measured along the curve of the scansor's base from the base of the distalmost seta to the base of the proximalmost seta. The number of setal rows was counted as the number of rows present in the sagittal section. Setal length was measured for each unobstructed seta by tracing the midline of the curve of the seta, from its base to the distal extremity of the setal tips. Setal diameter was measured at a height of approximately 5–15 μm from the base of the seta. Mean values of length and density were calculated only if the majority of setae from all areas of the scansor were visible and able to be measured. Setal density was calculated as the number of setae mm^{-2} and was determined by squaring the number of setal rows along a 32-μm length of the scansor, giving a density of setal stalks per 1000 μm^2 (Fig. 2), based upon the observation that setal spacing is approximately equal for both ranks (anteroposteriorly along a scansor) and rows (mediolaterally across a scansor) of setae (Delannoy, 2006). This value was then multiplied by 1000 to obtain an estimate of setal density mm^{-2}, and calculated for the proximal, intermediate and distal regions of each scansor examined, trends observed, and mean values calculated. Setal resting angle was measured as the angle between the setal shaft and the surface of the scansor.

Other measurements calculated for comparison include the change in setal length along a scansor (the length of the distalmost seta minus the length of the proximalmost seta), and the estimated detachment angle of the scansor. Scansor detachment angle was calculated using scansor length and the change in setal length along the scansor to determine the angle to which the scansor must be raised for setae to simultaneously reach an identical angle (in this case 30°, based upon previously published information about the critical detachment angle observed for *G. gecko*; Autumn et al. 2000) relative to a flat surface. This estimated angle relates to the gradational length of the setae on each scansor and along the digit. As the scansor is raised to a certain angle relative to the surface, the differential length of the setae along the scansor results in them being raised to an identical angle. This would promote simultaneous detachment of all setae

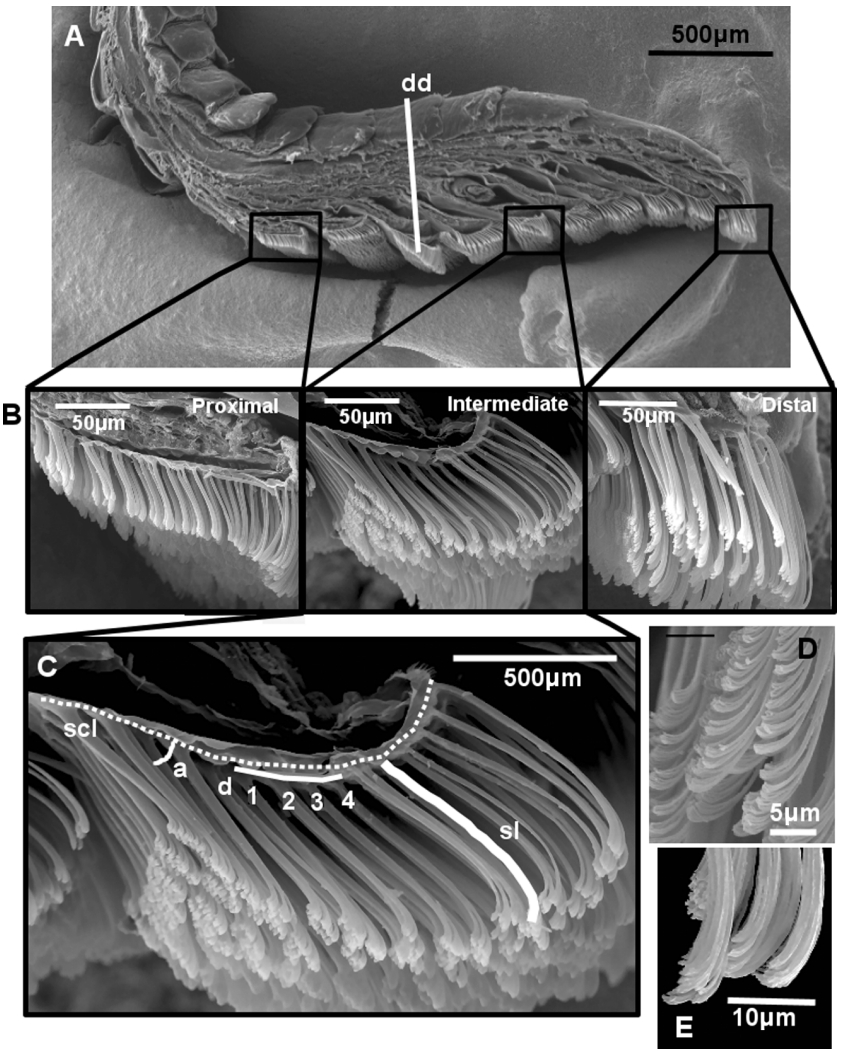

Fig. 2 SEM images showing digit morphology, scansor location, setal morphology and measurements taken (*Rhoptropus diporus* is shown). (A) Sagitally sectioned digit showing the general anatomical location of the proximal, intermediate and distal scansors examined. dd, Measurement of digit depth taken at the deepest region of the pad. (B) Magnified view of the proximal, intermediate and distal scansors showing the difference in general configuration. (C) Measurements taken for each scansor: sl, measurement of setal length taken along the midline of the seta from base to tip; d, Measurement of setal density. The horizontal white line represents 32 µm; the number of setae along this line was counted and squared to give setal density per 1000 µm^2, scl, measurement of scansor length – dashed line; a, measurement of setal resting angle. (D) Morphology of proximally located setae and (E) morphology of distally located setae.

on the scansor at a particular critical angle. Although an angle of 30° was employed in our calculations (see above), the actual angle that is critical for each species need not be 30°. The important factor here is that because of the graded lengths of the setae on a scansor (longest distally, shortest proximally) an identical critical angle will be obtained simultaneously by all setae on the scansor. This would not occur if setal length did not vary along the length of the scansor. The estimated scansor detachment angle, therefore, reflects this morphological pattern of setal arrangement, and explores the principle of the design rather than any explicit detachment angle.

Conventional statistical analysis

Comparisons across species are problematic due to the fact that species cannot be considered as independent units because of their shared ancestry (Felsenstein, 1985; Harvey & Pagel, 1991; Martins & Garland, 1991). Conventional statistical methods are rendered invalid if a 'phylogenetic effect' exists between species; that is, if sister taxa are similar due to their shared ancestry. However, for the purpose of determining simply whether differences between species exist, and not whether these differences are specifically and causally correlated with some other factor, conventional statistics can be used (Silvertown & Dodd, 1996) as long as it is understood that the similarities or differences revealed are likely due to a combination of phylogenetic and ecological effects. Thus, a series of conventional comparative analyses was carried out to first establish the general trends across species. Phylogenetic tests were subsequently conducted, and are described in the next section. Comparisons within each species were also performed using conventional statistical methods. All conventional statistics were conducted using Microsoft Excel 2003 and SYSTAT V.12.00.08 (Wilkinson, 2007).

Series of paired *t*-tests were conducted to evaluate patterns within each species, for maximum and minimum setal lengths and setal diameters for each scansor, and for mean setal length, diameter and density between different scansors. The alpha value used to assess significance of each test was determined using a Bonferroni adjustment based on an initial alpha value (0.05) and the number of comparisons made (15) to take into account multiple comparisons. The assumption of normality of the data was tested prior to analysis using Kolmogorov–Smirnov Lilliefors tests. Where paired *t*-tests were not performed, general trends were observed.

The least squares model of regression was used to explore relationships between setal measurements and the size (mass) of the animal. The morphological data were log-transformed prior to

Table 1 Nei's (1978) genetic distance data and distance classes for the calculation of Moran's I for *Rhoptropus* species and *Chondrodactylus bibronii* (adapted from Bauer & Good, 1996). The distance class of each species pair is shown in brackets, and represents the following ranges of genetic distances: (1) 0–0.25, (2) 0.25–0.5, (3) 0.5–0.75, (4) 0.75–1.0, (5) 1.5–1.75, (6) 2.0–2.25

Species	*R. biporosus*	*R. barnardi*	*R. boultoni*	*R. bradfieldi*	*R. afer*	*C. bibronii*
R. biporosus	–	0.182 (1)	0.460 (2)	0.715 (3)	0.979 (4)	1.60 (5)
R. barnardi		–	0.214 (1)	0.461 (2)	0.850 (4)	1.60 (5)
R. boultoni			–	0.674 (3)	1.037 (4)	1.60 (5)
R. bradfieldi				–	0.608 (3)	1.62 (5)
R. afer					–	2.07 (6)
C. bibronii						–

analysis to normalize the distribution of the data, and regressions performed to determine the relationship of each variable to body size (mass). If the regression was found to show a significant relationship between the variable and body mass ($P < 0.05$), the residuals of the regressions were recorded to obtain a size-free dataset (Garland et al. 1992; Albrecht et al. 1993) to be used in subsequent analyses. For variables found to be unrelated to size, the original log-transformed values were included in the size-free dataset, rather than the residuals.

Principal component analysis (PCA) was used to assess the major sources of variation in the data (Pimentel, 1979; Karlis et al. 2003). Three separate correlation matrix (Pimentel, 1979) PCAs were performed: one for each scansor examined (distal – PCA I, intermediate – PCA II, and proximal – PCA III). Each of the three PCAs used the size free datasets, as described above, included all seven species of *Rhoptropus* plus *C. bibronii,* and incorporated the following measurements: pad area, scansor length, number of setal rows, maximum, minimum and mean setal lengths, maximum and minimum setal diameters, distal, intermediate, proximal and mean densities, and estimated detachment angle of the scansor. Specimens with missing data were removed prior to analysis. Informative principal components (PCs) were determined using the Kaiser criterion, which defines them as PCs in a correlation matrix with eigenvalues greater than one (Karlis et al. 2003). To facilitate interpretation, the PCAs were subjected to a varimax rotation, which results in each component being associated with only a few variables with very high loadings (Kaiser, 1958). Factor scores for informative PCs of each PCA were collected, and these scores, which represent the values of each specimen for the 'new' variables (PCs), were used in subsequent analyses.

Analyses of variance (ANOVAS) were conducted to test for differences between the factor scores obtained, as described above. The normality assumption of ANOVA was tested using Kolmogorov–Smirnov Lilliefors tests, and homogeneity of variance was tested using Levene's test (Schultz, 1985). Separate analyses were performed for each informative PC from each of the three PCAs (distal, intermediate and proximal scansors), with the data being grouped by species to determine which, if any, species demonstrate differences in their setal dimensions and patterns. In the case of significant ANOVAS ($P < 0.05$), Tukey's pairwise comparisons were used to determine which species actually differ from the others.

Discriminant function analysis (DFA) is used to further explore the results revealed by the PCAs. Three forward-stepping DFAs were performed, one for each of the scansors investigated (distal – DFA I, intermediate – DFA II, and proximal – DFA III) using the same measurements listed above for the PCAs. The forward-stepping DFAs were carried out with an F-to-enter (the minimum F value required by a variable to be included in the DFA model) of 4.00, and an F-to-remove variable of 3.90. Significance of the contribution of each variable to the DFA model, and therefore its ability to discriminate between species groups, was determined using the Wilk's lambda statistic (Cocozzelli, 1988).

Phylogenetic statistical analysis

The Moran's I (Moran, 1950) statistic is commonly used to assess spatial autocorrelation of traits in animals across a particular habitat (Cliff & Ord, 1973, 1981). However, it has also been adopted for assessing phylogenetic autocorrelation using phylogenetic distance data (Gittleman & Kot, 1990). Moran's I was calculated as described by Gittleman & Kot (1990) for PCA factor scores showing significant difference between species, which included factor scores of PC1 and PC3 from PCA I and PCA II, and PC1 and PC4 from PCA III . These variables were used to determine whether the significant results obtained for them may be due, in part, to phylogenetic effects. Moran's I was calculated for all *Rhoptropus* species (with the exception of *R.* cf. *biporosus* and *R. diporus*) plus *C. bibronii*, which were grouped into six distance classes using the Nei's (1978) genetic distance data derived from allozymes by Bauer & Good (1996). These distance classes are shown in Table 1. Using these groups, correlograms of Moran's I and their associated z-scores were created.

Phylogenetic analysis of variation by computer simulation using the PDAP V.5. package (Garland et al. 1993) was also employed to evaluate species differences in a way that takes into account phylogenetic effects. This method requires that mean values for species are used, and therefore it cannot be used to compare individual species, but can be used to assess differences between groups of species showing different ecological characteristics (Garland et al. 1993). One trend within *Rhoptropus* is the adoption, when compared to other species, of a more terrestrial lifestyle by *R. afer* (Bauer et al. 1996; Johnson et al. 2005); therefore, this method was used to compare species demonstrating a climbing lifestyle with species having a more terrestrial lifestyle (*R. afer*). This method was conducted as described by Garland et al. (1993) using the mean values of PCA factor scores found by conventional ANOVAS to reveal any differences between *R. afer* and the other species (see Results section). The analysis was conducted using both constant branch lengths (Martins & Garland 1991) and a set of actual branch lengths, representing the number of base-pair differences between the species (Bauer & Lamb 2005; Lamb & Bauer, unpublished); *R.* cf. *biporous* was estimated to have diverged halfway along the branch to *R. biporosus* and to show the

same amount of genetic change as its sister species. In all, 1000 simulations were conducted for the factor scores under the assumption of a speciational Brownian model of evolution with no boundaries.

Results

Setal morphology, patterns and variation within species

Setal length and other dimensions show a great deal of variation both across species and within individuals. Across all species and all scansors examined, setal length was found to range from a minimum of 15.7 μm (at the proximal end of the proximalmost scansor of *R. afer*) to a maximum of 103 μm (at the distal end of the distalmost scansor of *R. bradfieldi* and *C. bibronii*), and setal diameter from a minimum of 1.23 μm (at the proximal end of the proximalmost scansor of *R. diporus*) to a maximum of 5.7 μm at the proximal end of the intermediate scansor of *R. barnardi*). Average setal length and diameter across all species and across all regions of the digit was approximately 60 μm and 2.8 μm, respectively. Variation in setal dimensions across scansors and between species is discussed below.

Examination of all species revealed a pattern of setal field arrangement and morphology that was universal. Along a generalized scansor (one in an intermediate location on the digit) setal morphology changes dramatically from the distal to the proximal end. Setae at the distal end of the scansors are long, slender, and branch profusely at about the midpoint of the length of the seta from its base (Fig. 2C). Most of the branches are of approximately the same length, and they curve toward the proximal end of the scansor (Fig. 2C). Moving towards the proximal end of the scansor, setae become gradually shorter and thicker, with the progressively shorter setae fitting into the curve of the preceding longer seta (Fig. 2C). Furthermore, although the initial point of branching remains at approximately 50% of the length of the shaft, branches of the setae are of differential length, and all curve proximally, with shorter branches fitting in against the curve of the longer branches (Fig. 2C). These patterns are also observed on the distalmost scansor, and on all other intermediate scansors in specimens for which all scansors were examined, but they break down to some extent at the proximal end of the proximalmost scansor, where structures become shorter and less branched (Fig. 2B).

The trends of decreasing setal length and increasing diameter from the distal to the proximal end of each scansor are evident in each species (Figs 3, 4). The pattern is quite clear and regular for setal length, but fairly erratic

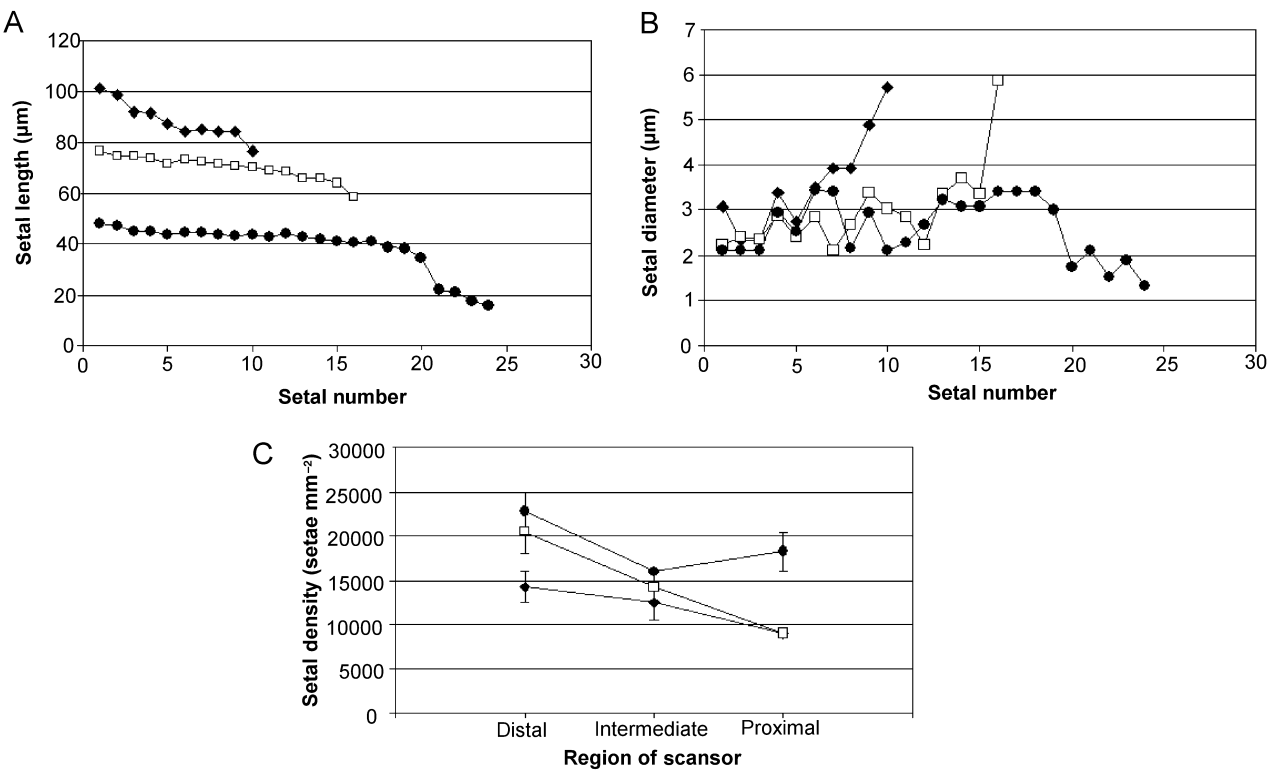

Fig. 3 Graphs showing the general trends in setal dimensions along a distal (black diamonds), an intermediate (open squares) and a proximal (black circles) scansor in a representative specimen of *Rhoptropus boultoni.* Trends are shown for (A) setal length, (B) setal diameter and (C) setal density. Note the decrease in setal diameter and increase in density at the proximal end of the proximalmost scansor. Trends are similar for all other species of *Rhoptropus*, and for *Chondrodactylus bibronii.*

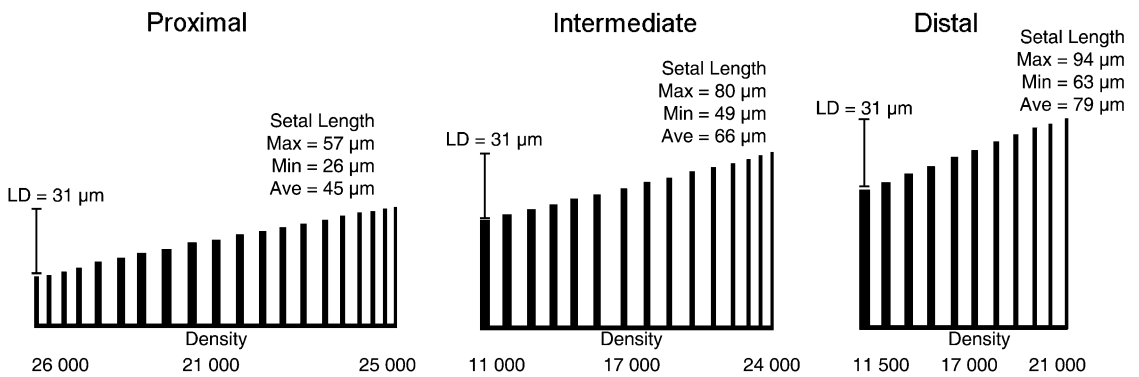

Fig. 4 Schematic diagram showing common trends in setal field configuration and dimensions across generalized proximal, intermediate and distal scansors of *Rhoptropus.* Across all scansors these trends include: decreasing scansor length and number of setal rows (from 20 to 10) distally, an overall increase in setal length distally, an unchanging pattern of setal diameter and setal length difference (LD) for all scansors, and higher setal density proximally. For each individual scansor trends include: increasing length and decreasing diameter distally, and increasing density distally (except for the proximal scansor). All measurements given are averaged across all specimens examined; Setal density is in units of setae mm^{-2}. All lengths in the diagram are shown to scale.

for setal diameter, which varies within a small range and shows only a very general trend of increase along the length of the scansor. These results are also supported by the results of the paired *t*-tests for each species (see Supporting Information), which reveal that the difference between maximum and minimum setal length on a scansor is significant for several species, with many others exhibiting comparisons that were nearly significant. Similarly, several species show a significant trend of decreasing setal diameter along each scansor from proximal to distal. The exception is the proximal scansor, for which some species (*R. afer, R. boultoni* and *R. diporus*) show a decrease in setal density at the proximal end, where setal structure begins to break down. On the distal and intermediate scansors, setal density decreases from the distal region to the proximal region. This trend continues on the proximal scansor in *R. barnardi* and *R. biporosus*, but in the remaining species setal density increases at the proximal end of the proximal scansor rather than decreasing further (Figs 3, 4).

Taken as individual units, each scansor demonstrates a similar set of trends; however, there are also trends between scansors that are common to all of the species investigated, with variation occurring from one scansor to the next. Two of these trends are an increase in scansor length moving from the distalmost scansor proximally and, related to this, a general increase in the number of setal rows present on the scansor (Fig. 4).

Trends in setal length are also apparent, with mean setal length increasing from one scansor to the next, moving from the proximal to the distal end of the digit. Observations of setal length for all scansors of one specimen of every species also support this trend, showing that it is consistent across all of the scansors. Results of the paired *t*-tests reveal that the trend is not strongly statistically significant (see Supporting Information Table S2). Maximum and minimum setal lengths were observed to follow similar trends to mean setal length, with both the longest and the shortest setae becoming gradually shorter from the distalmost scansor proximally. However, the difference between maximum and minimum setal length remains very constant from one scansor to the next (Fig. 4).

Setal diameter (mean, maximum and minimum) does not follow a clear pattern, and stays relatively constant between scansors. The same is true for mean setal density, which does not change greatly between scansors, except for an increase on the proximal scansor (Fig. 4) that is noticeable in *R. bradfieldi*, *R. diporus* and *C. bibronii*, but only significant for *C. bibronii* (see Supporting Information Table S2).

Setal tip morphology was not easily examined due to the quality of the specimens, and was observed for only one or two specimens of most of the species examined (*R. afer*, *R. barnardi*, *R.* cf. *biporosus*, *R. boultoni* and *R. bradfieldi*). Overall, the setal tips in all species ranged in diameter from about 0.10 to 0.20 µm, with approximately 300–400 tips per seta on distal or intermediate setae. Proximal setae on each scansor possess a larger number of tips (up to 900–1000 tips per seta). Based on values of mean setal density across all species of about 20 000 setae mm^{-2} for the distal and intermediate portions of a scansor, and about 10 000 setae mm^{-2} for the proximal region, the values for setal tip density are 6.0×10^6–8.0×10^6 and 9.0×10^6–1.0×10^7 tips mm^{-2} for the distal/intermediate and proximal regions of the scansor, respectively.

Setal patterns and variation between species

In general, all species show the same pattern of setal field arrangement and morphology described above. The species

Table 2 Eigenvalues and the percent of variance explained by each principal component from three principal component analyses. PCA I includes measurements from the distalmost scansor, PCA II from an intermediate scansor, and PCA III from the proximalmost scansor. See text for a complete list of measurements included in each test. Eigenvalues of informative components (as determined by the Kaiser criterion; Karlis *et al*. 2003) are marked with an asterisk

	PCA I		PCA II		PCA III	
Component	Eigenvalue	% variance	Eigenvalue	% variance	Eigenvalue	% variance
1	4.233*	28.219	4.936*	32.908	4.73*	31.532
2	2.987*	19.916	3.163*	21.088	2.838*	18.922
3	2.122*	14.145	1.508*	10.052	2.407*	16.044
4	3.144*	8.958	1.346*	8.971	1.647*	10.977
5	1.138*	7.584	1.057*	7.047	0.856	5.708
6	1.018*	6.789	0.971	6.477	0.806	5.375

Table 3 Degrees of freedom (df), *F*-ratio and *P*-value results of ANOVAS comparing factor scores of informative components (PCs) from three PCAs. PCA I, distal scansor; PCA II, intermediate scansor; PCA III, proximal scansor. Significant *P*-values are marked with an asterisk

	PCA I			PCA II			PCA III		
PC factor	df group; error	*F*	*P*	df group; error	*F*	*P*	df group; error	*F*	*P*
Scores									
1	7, 16	5.041	0.004*	7, 21	3.680	0.009*	7, 23	3.171	0.017*
2	7, 16	1.888	0.139	7, 21	1.990	0.105	7, 23	2.589	0.040*
3	7, 16	5.748	0.002*	7, 21	8.504	0.000*	7, 23	3.092	0.019*
4	7, 16	1.328	0.300	7, 21	0.610	0.742	7, 23	5.602	0.001*
5	7, 16	1.855	0.145	7, 21	1.952	0.111	–	–	–
6	7, 16	0.568	0.771	–	–	–	–	–	–

do, however, differ greatly in terms of absolute size, ranging from very small animals with average masses under 2 g, including *R. barnardi* (1.4–1.7 g), *R. afer* (1.4–2.5 g), *R. biporosus* (1.3–2.3 g) and *R.* cf. *biporosus* (1.5–2.9), to larger *Rhoptropus* species such as *R. bradfieldi* (2.9–4.3 g), *R. boultoni* (4.6–5.8 g), and *R. diporus* (0.9–4.7 g) with average masses between 3 and 5 g, to *C. bibronii*, which has an average species mass of 13 g (range 1.7–24.6 g). The three representative scansors chosen for investigation (distalmost, intermediate, and proximalmost) are associated with the same or similar anatomical regions of digit IV in all species, regardless of digit size or total scansor number, suggesting that they are functionally similar units (Fig. 2A).

The results of the PCAs on the size-removed datasets (Table 2 and Supporting Information Table S3) reveal the following. The first six components were found to be informative for PCA I (distal scansor), the first five components for PCA II, the first four components for PCA III (Table 2). For all three PCAs the first three components explained most of the variation, with PC1 explaining around 30%, PC2 around 20% and PC3 10–15% of the variation in the data. For PCA I, the component loadings (see Supporting Information Table S3) suggest that PC1 represents variation in setal length, PC2 represents variation in setal density, and PC3, PC4, PC5 and PC6 represent variation in pad area and scansor number, scansor length and number of setal rows, hyperextended scansor detachment angle, and digit depth, respectively. Results are similar for PCA II, with PC1 representing setal length, PC2 representing scansor length and the number of setal rows, PC3 representing pad area and total number of scansors, PC4 representing digit depth, and PC5 representing intermediate setal density. For PCA III, PC1 once again represents setal length, PC2 represents scansor length and the number of setal rows, PC3 represents setal density, and finally PC4 represents variation in pad area and total number of scansors (see Supporting Information Table S3). Plots of factor scores (Fig. 5) for each informative PC show clustering patterns of the species with respect to the different components. Species show a great deal of overlap for many of the components, with very few clear clustering patterns. However, some patterns are apparent; for both PCA I and PCA II *R. afer* is separated from the other species along PC1, and *R. afer* and *R.* cf. *biporosus* show some separation from the other species along PC3 and along PC4 for PCA III.

Results of conventional ANOVAS comparing factor scores from each PCA support the results seen in the factor score plots described above (Table 3). Differences between species are significant for the factor scores of PC1 and PC3

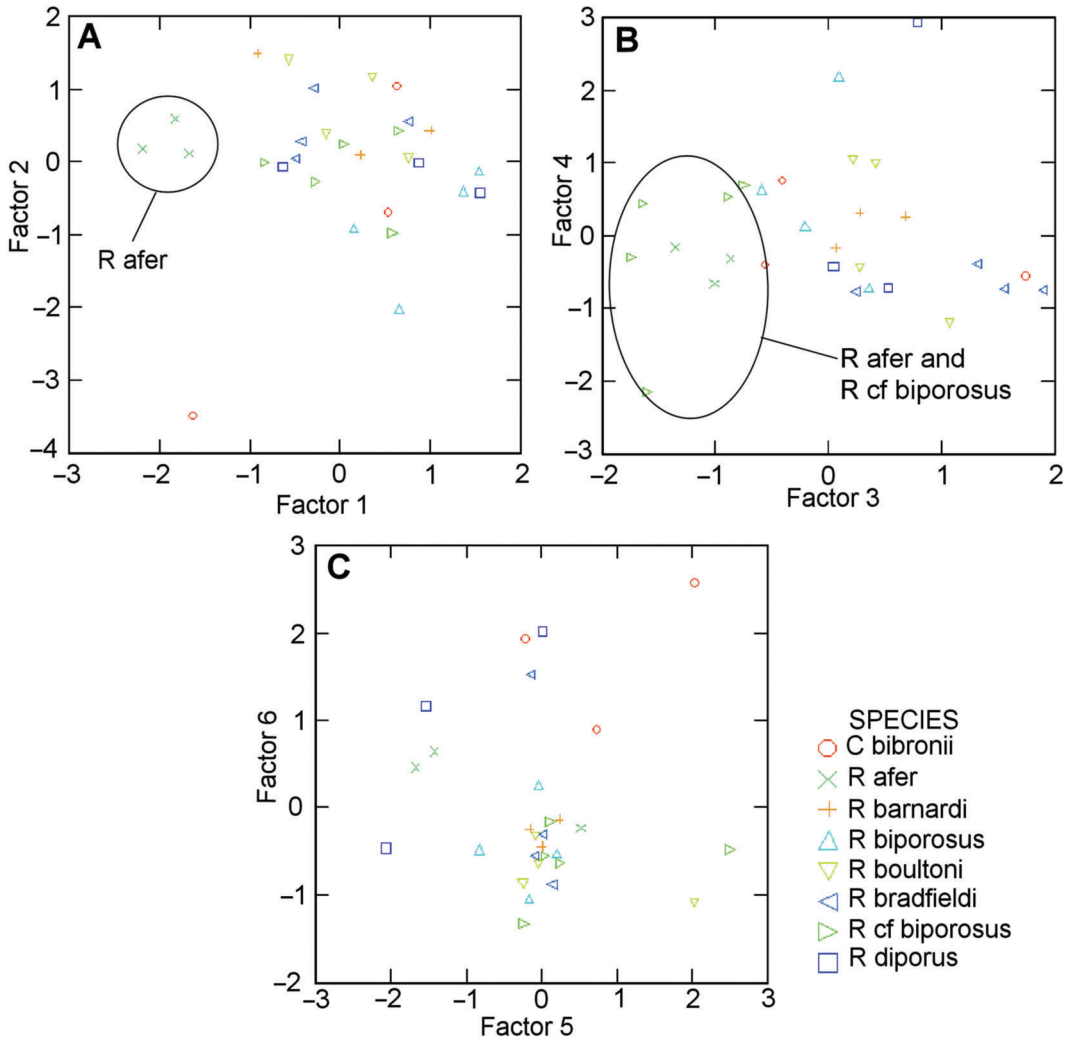

Fig. 5 Plots of factor scores of PCA II (intermediate scansor measurements) for all examined species of *Rhoptropus* and *Chondrodactylus bibronii*. The plots show clustering patterns of species with respect to (A) principal components 1 and 2, (B) PC3 and PC4 and (C) PC5 and PC6. Patterns for PCA I (distal scansor) and PCA III (proximal scansor) are similar.

for PCA I and PCA II, and for all four PCs of PCA III (although only barely significant for PC2). Tukey's multiple comparisons tests revealed that the significant differences for PC1 can be attributed to differences between *R. afer* and all other *Rhoptropus* species for PCA I; between *R. afer* and all other *Rhoptropus* species except *R. barnardi* and *R. bradfieldi* for PCA II; and between *R. afer* and *R. biporosus* for PCA III ($P < 0.05$). Differences in PC3 factor scores are attributable to differences between *R.* cf. *biporosus* and *C. bibronii*, *R. bradfieldi*, *R. boultoni* and *R. diporus* for PCA I, and between these same species as well as between *R. afer* and *R. boultoni* and *R. bradfieldi* for PCA II (Tukey's test, $P < 0.05$). PC4 of PCA III is comparable to PC3 of the other two PCAs in terms of the measurements it represents, and differences in its factor scores for PCA III are attributed to similar species differences, including those between *R.* cf. *biporosus* and *C. bibronii*, *R. bradfieldi*, *R. boultoni* and *R. diporus*, as well as between *R. afer* and *R. boultoni* and *R. bradfieldi*, *R. diporus* and *C. bibronii* (Tukey's test, $P < 0.05$). Finally, the differences in the factor scores associated with PC2 from PCA III cannot be attributed to any significant differences between species (Tukey's test, all $P > 0.05$), and those of PC3 are attributed only to a difference between *C. bibronii* and *R. boultoni* (Tukey's test, $P < 0.05$).

The DFAs revealed trends in the data very similar to those obtained from the PCAs. For DFA I, two variables met the F-to-enter criterion of 4.00 and were included in the discriminant function model – maximum setal length on the distal scansor, and pad area. The Wilk's lambda values for these two variables were 0.122 and 0.023, respectively, both of which are highly significant ($P < 0.001$). The ability of the DF model to predict the membership of each specimen in its correct species is shown in Table 4.

Table 4 Jack-knifed classification results from discriminant function analyses (DFAs) showing the ability (% correct) of the discriminant function model to correctly predict species membership for (a) DFA I (distal scansor), (b) DFA II (intermediate scansor) and (c) DFA III (proximal scansor)

	% correct classification		
Species	DFA I	DFA II	DFA III
R. afer	100	100	67
R. barnardi	0	33	0
R. biporosus	33	25	33
R. cf. *biporosus*	60	80	50
R. boultoni	25	75	25
R. bradfieldi	0	25	67
R. diporus	0	0	67
C. bibronii	0	67	56
Total	54	52	48

Table 5 Results of the phylogenetic analysis of variance (ANOVA) on factor scores of principal components from three PCAs. The ANOVAS compare climbing *Rhoptropus* species and those showing increased terrestriality (*Rhoptropus afer*). The *F*-values are from conventional ANOVAs, and the critical *F*-value to which they are compared is derived from an empirical *F*-distribution constructed by computer simulation of the characters along the tree in Fig. 1. The critical *F*-values found using constant branch lengths and real branch lengths are shown. Significant *F*-values are marked with an asterisk

				Critical *F*-values	
PCA	PC	*F*-value	df group; error	Constant branch lengths	Actual branch lengths
I	1	28.694*	1, 22	5.300	4.664
	3	1.858	1, 22	5.376	4.323
II	1	19.824*	1, 27	5.244	4.847
	3	4.321*	1, 27	4.093	4.720
III	1	5.211*	1, 29	4.561	4.533
	3	9.094*	1, 29	5.689	5.173

The model is able to correctly predict the membership for *R. afer* 100% of the time, and *R.* cf. *biporosus* 60% of the time, but performs less well for the other species. The model also established two new variables (canonical discriminant functions), the first of which explains 86% of the variation between species, and the second the remaining 14%. The first discriminant function is explained primarily by maximum setal length and the second discriminant function is largely based on variation in pad area.

For DFA II, three variables were added to the model: pad area, maximum setal length and minimum setal length on the intermediate scansors. The Wilk's lambda values associated with each variable are 0.204, 0.055 and 0.014, which are all highly significant ($P < 0.001$). The model for DFA II was also able to correctly classify *R. afer* and *R.* cf. *biporosus* a high percentage of the time (Table 4), but was also fairly successful at classifying *C. bibronii* and *R. boultoni.* The three canonical discriminant functions explain 64%, 26% and 9% of the variation between species, respectively, with the first being associated with all three variables, the second with minimum setal length and the third with maximum setal length.

The results for DFA III are similar, with three variables (average and minimum setal length, and pad area) being included in the analysis (Wilk's lamba 0.303, 0.124 and 0.048, respectively, $P < 0.001$). Using these measurements, the model for DFA III was able to classify *R. afer*, *R. bradfieldi* and *R. diporus* with 67% correctness (Table 4). The three canonical discriminant functions explain 50%, 29% and 11% of the variation between species, respectively. Once again, the first discriminant function is represented by all three variables, the second by minimum and average setal length, and the third by minimum setal length.

Calculation of Moran's I statistics resulted in associated *z*-scores that revealed some phylogenetic autocorrelation between the species for the measurements and factor scores considered (Fig. 6). Significant levels of positive autocorrelation were found for the first distance class for two of the variables examined. Other significant values were negative, suggesting that the phylogenetic distance between the species is at least somewhat responsible for the differences between species (Gittleman & Kot, 1990; Epperson & Chung, 2001). Significant levels of negative autocorrelation are found mostly in distance classes 3, 4, and 6, all of which contain species pairs including *R. afer.* This suggests that *R. afer* is markedly different from the other species for some of these variables, and that this difference is at least partially attributable to phylogeny, and, in particular, its genetic distance from other species in its clade.

The results of the phylogenetically corrected ANOVAS comparing *R. afer* to the other *Rhoptropus* species and *C. bibronii* indicate that the significant difference of *R. afer* seen in the results of the conventional analyses remains valid even when phylogeny is taken into account (Table 5). *Rhoptropus afer* differed significantly from the other species for the factor scores of PC1 from PCA I, PC1 and PC3 from PCA II and PC1 and PC4 from PCA III. For the most part, however, both the actual and constant branch lengths yielded very similar results (Table 5).

Discussion

Setal field configuration – functional implications

The pattern of setal arrangement into setal fields, and the geometry of the setae themselves are essential data for the determination of the strength of contact and attachment that can be achieved by the subdigital adhesive system.

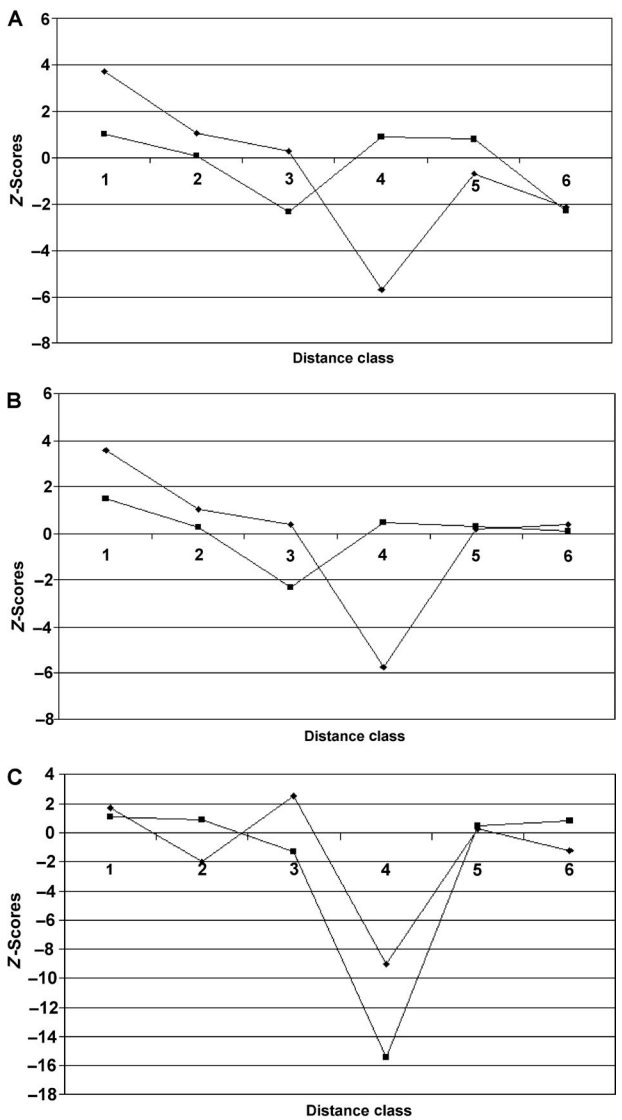

Fig. 6 Phylogenetic correlograms showing the degree of phylogenetic autocorrelation across six distance classes of *Rhoptropus.* Phylogenetic autocorrelation is shown by z-scores calculated from Moran's I statistics for (A) factor scores of PC1 (diamonds) and PC3 (squares) from PCA I (distal scansor), (B) factor scores of PC1 (diamonds) and PC3 (squares) from PCA II (intermediate scansor), and (C) factor scores of PC1 (diamonds) and PC4 (squares) from PCA III (proximal scansor). See text and Table 1 for explanation of distance classes.

The adhesive system of geckos functions by way of a highly controlled mechanism, and the manner in which effective substratum contact is made is likely through the initial formation of van der Waals bonds as setae are pushed into the surface, followed by the activation of shear forces as setae are loaded in tension (Autumn et al. 2000, 2002, 2006; Autumn & Peattie, 2002; Tian et al. 2006). The dependence of the adhesive system on van der Waals bonding implies that there is a direct relationship between setal geometry and adhesive capabilities, with the shape and size of attachment devices being much more important than the chemical composition of the structures (Autumn et al. 2002; Spolenak et al. 2004; Guo et al. 2007). The importance of tip diameter and density has been extensively investigated, as these dimensions are critical for the determination of the amount of potential contact with the substratum at the nano-scale, and thus the amount of force that can be generated (Arzt et al. 2003; Persson, 2003; Peressadko & Gorb, 2004). However, although contact and adhesion at the nano-scale are important, the overall configuration of setal fields and setal geometry ultimately govern the potential for interaction between the subdigital pads and the surface, and in placing the setal tips into an orientation that allows contact in the first place.

Setal field configuration is a subcomponent of the structure of the digits themselves and their mode of operation. The arrangement of a set of setae on the digit determines how they can be brought into, and removed from, contact with the substratum. Setal fields are not homogeneous in structure because local anatomical associations determine local patterns of interaction and deployment. Variation in any aspect of setal morphology, including length, diameter and density, will have implications for the functional role of the structures (Delannoy, 2006). This is especially important in the deployment of setae, which requires setae to be brought into contact with the substrate in the proper orientation (Autumn et al. 2002). The ability to generate maximal adhesive force is thus highly influenced by the pattern arrangement and dimensions of the adhesive structures in relation to both substratum configuration and anatomical position.

Overall, the pattern of setal field configuration observed in *Rhoptropus* is comparable to that of the Tokay gecko (*G. gecko*), with the region of the digit observed in *Rhoptropus* corresponding to the region described by Delannoy (2006), which includes scansors associated with the lateral digital tendon system. Like those of *G. gecko*, the setae of *Rhoptropus* in this area of the digit show characteristics typical of those described in the literature, being fairly long, highly branched, and terminating in spatular tips (Ruibal & Ernst, 1965; Maderson, 1970; Autumn et al. 2000, 2002; Hansen & Autumn, 2005; Guo et al. 2007). Although setal tip parameters could not be determined for all specimens of *Rhoptropus,* estimates of setal tip density in *Rhoptropus* of 6.0×10^6–1.0×10^7 tips mm^{-2} are similar to values of 3.8×10^6–9.0×10^6 tips mm^{-2} obtained for *G. gecko*, suggesting that the setal tips of *G. gecko* are not more profusely branched than are those of *Rhoptropus.* Measurements of setal tip diameter for *Rhoptropus* of 0.10–0.20 μm are also very much in line with values obtained for *G. gecko*, possibly representing conserved size of setal tips, or perhaps a physical limitation of splitting that the setal tips can undergo.

All in all, the conservation of general setal field patterns across distantly related groups (*Gekko* and *Rhoptropus*), as well as across the *Rhoptropus* radiation, suggests that this overall pattern of configuration has important functional implications. Although variation exists at the species level for some setal dimensions, the overall configuration and pattern remains consistent for all species examined. This is the case for patterns observed between two species of the genus *Gekko*, *G. gecko* and *Gekko swinhonis* (Günther 1864), in which characteristics of overall setal field arrangement are similar, although subtleties of branching pattern and setal tip arrangement apparently vary between the two species (Guo et al. 2007). Whether the tip configurations are consistently different or not is at present unclear because Guo et al. (2007) were not explicit about how the setae were sampled, and from which region of the digit the setae came. This issue is discussed in more detail in the conclusions.

The length of the setae has important implications for their mechanical properties. Although length varies along the digit and along the scansors, setae are, in general, relatively long compared to the epidermal outgrowths that invest the rest of the body, which are about 1–2 μm in length (Stewart & Daniel, 1972; Delannoy, 2006). Longer structures require less force to bend them because they present longer lever arms (Vogel, 2003). Setae must be depressed below 30° for proper adhesion to occur, and, as such, long setae may be able to be loaded properly with less energy expenditure. Conversely, shorter setae at the proximal end of each scansor and at the proximal end of the digit would be more rigid and would bend less easily. The tendency for longer setae at the distal end of each scansor to have a smaller diameter than the shorter setae at the proximal end enhances this pattern, as short, thick setae have a smaller aspect ratio than longer, thinner setae, and would be much less compliant. According to beam theory, a structure's resistance to bending, its 'bending stiffness', decreases substantially as length increases, but is augmented by increasing radius. Bending stiffness (K) can be described by eq. 1 (from Autumn et al. 2006b), where E is the elastic modulus, r is the radius and L is the length of the structure.

$$K = (3\pi Er^4)/(4L^3) \quad (1)$$

Assuming that setal β-keratin has an elastic modulus of approximately 1 GPa (Persson & Gorb, 2003; Autumn et al. 2006b), long, slender structures at the distal end of the distalmost scansor would have an average bending stiffness of 1.34×10^{-6}–4.74×10^{-6} N m^{-1} (calculated as per Autumn et al. 2006b) across all species of *Rhoptropus*, whereas shorter, thicker structures at the proximal end of the same scansor have values of bending stiffness of 2.45×10^{-3}–9.48×10^{-3} N m^{-1}, three orders of magnitude lower than the longer setae.

It is known, however, that the form of setae as high aspect ratio shafts causes them to behave differently than does bulk β-keratin, with a much lower effective elastic modulus (E_{eff}) than the 1 GPa estimated above (Autumn et al. 2006b). This is important as an E_{eff} of less than 100kPa is required for setae to function as pressure sensitive adhesives (PSAs) and to adhere effectively to surfaces (Autumn et al. 2006b). The effective elastic modulus is also influenced by setal length and radius, with longer, thinner structures having a lower effective elastic modulus, and thus less bending stiffness, than that calculated above. Effective elastic modulus (E_{eff}) can be calculated using eq. 2 (from Autumn et al. 2006b), where E is the elastic modulus (1 GPa), I is the moment of inertia ($I = \pi R^4/4$), D is the density of setae (1.44×10^{10} m^{-2}; Autumn et al. 2006b), φ is the resting angle of the setae, L is setal length, and μ is the coefficient of friction (0.25; Autumn et al. 2006b).

$$E_{eff} = 3EID\sin(\varphi)/L^2\cos^2(\varphi)[1 + \mu\tan(\varphi)] \quad (2)$$

The setae of the *Rhoptropus* species examined herein consistently demonstrate an average resting angle of 45° for setae located proximally on a scansor and 80° for setae located at the distal end. Based on this, setae at the distal end of the distalmost scansor have a very low effective elastic modulus of 0.8–2.85 kPa, and, therefore, an effective bending stiffness of only 1.06×10^{-12}–1.35×10^{-11} N m^{-1}, whereas setae at the proximal end of the scansor have a much higher E_{eff} of 2612–2747 kPa (which is still lower than the estimated 1GPa, but higher than the 100 kPa required for PSAs), and a bending stiffness of 6.41×10^{-6}–7.27×10^{-5}.

The relatively greater rigidity of the shorter, proximally located structures has important implications for attachment. Recent studies have focused on the importance of frictional or shear forces in addition to van der Waals bonding for the establishment of maximum setal force (Autumn et al. 2006a; Tian et al. 2006). At the microscopic level, both of these forces depend upon maximizing the area of contact (Bowden & Tabor, 1966; Autumn et al. 2002), and thus long, flexible setae seem better suited to engendering this type of attachment, as shorter, thicker structures with their higher E_{eff} are less likely to achieve adhesive contact with the surface in the first place (Autumn et al. 2006b). At the same time, however, frictional load bearing requires the transmission of frictional forces by relatively immobile structures (Maderson, 1964), and thus shorter structures, which bend less easily, may be more suited to frictional interactions with the surface (Delannoy, 2006). However, as setae are loaded in tension (Peterson et al. 1982), the immobility of structures may be less important, allowing longer, more flexible structures to be involved in frictional interactions. The tensile strength of setae is also important here, as this is independent of the length of the setae, but is dependent on their cross-sectional diameter (Peterson et al. 1982). As such,

thicker setae may be important for their inherent tensile strength, but this does not explain the decrease in length associated with thicker setae. It is also possible that shorter, thicker setae are involved in some type of tractive interaction. Furthermore, at the level of the attaching tips, stiffness and E_{eff} may not differ between setae on different regions of the digit.

The variation in setal length along scansors and across the entire digit (Fig. 4) may have functional implications associated with adhesion on rough surfaces. While it seems that this variation may allow for increased contact with rough surfaces in the animal's natural environment (Persson, 2003; Peressadko & Gorb, 2004), with long setae being able to penetrate into asperities, and shorter stalks contacting more elevated areas of the surface, this is likely not the case. This would be effective if the surfaces encountered by these animals were very regular and predictable, as is the configuration of their setal fields, but these surfaces are, in reality, highly unpredictable (Russell & Johnson, 2007). Furthermore, it has been suggested that long, slender setae are ideal for attachment to rough surfaces (Campolo et al, 2003; Jagota & Bennison, 2002; Persson, 2003; Persson & Gorb, 2003; Meine et al. 2004; Spolenak et al. 2005; Autumn et al. 2006b). Long shafts held at a low angle relative to the surface have a high E_{eff}, allowing them to deform easily and comply with surface irregularities. However, these same properties promote matting of the setae (Persson, 2003; Glassmaker et al. 2004; Spolenak et al. 2005; Autumn et al. 2006b), which would compromise their adhesive capabilities (Stork, 1983). Therefore, the presence of shorter, stiffer setae would reduce the potential for matting, should this exist, and permit a greater packing density of setae (Spolenak et al. 2005). A combination of long and short setae may help to maximize adhesion in some areas while minimizing matting problems in others. Once again, however, this does not explain the predictable pattern of setal field organization.

One potential advantage of the regular pattern of setal length variation is the prevention of interference of setae with those in the adjacent row and on the adjacent scansor. Setal branches and setal shafts fit against the curve of the branch or stalk adjacent to them. When the system is deployed this would allow the setal tips carried on each branch of each shaft to attach to the substrate without interfering with the tips on adjacent branches, thereby allowing for maximization of contact with the substrate. This pattern continues at the level of the scansors. Scansors tend to overlap each other slightly, with the distal end of one scansor partially covering the proximal portion of the next, more distally located scansor. As a result, having shorter setae at the proximal end of one scansor would limit the interference between these setae and the longer setae at the distal end of the next scansor.

Finally, variation in setal length along the scansor may also play a role in facilitating detachment of the setae by way of its relationship to the angle of detachment of the scansor. When setae are deployed they are held at a low angle against the substrate (less than 30°) (Autumn et al. 2000). During detachment the digits are hyperextended, and rolled off the surface, resulting in the setae reaching the critical detachment angle of 30° (for *G. gecko*), at which they are released from the surface (Autumn et al. 2000; Russell, 2002). Setae of decreasing length along the scansor allow for the simultaneous detachment of all of the setae of an entire scansor because of the following: as the scansor is raised from the substrate, setae of various lengths will reach any given critical angle at the same time. If setae were of a constant length along a scansor then detachment would occur sequentially as each seta would reach 30° (or any other critical angle) at a different time, with the more distal setae detaching first. Simultaneous detachment of setae allows for quick and low energy release of the digits, facilitating rapid movement across substrates.

Whereas the absolute length of the setae changes from scansor to scansor, the absolute change in length along each scansor remains constant along the whole digit. This means that even as the length of the scansor and the number of setal rows increases proximally, the difference between the longest and shortest setae remains the same. Therefore, the difference in length between adjacent setae decreases as the repeated length differentials are spread across a larger number of setal rows. This implies that the length differential may have important functional attributes, and may allow for the most effective attachment and detachment of setal structures. An increase in scansor length in conjunction with the difference in setal length remaining constant also has implications for detachment. As a result of this, longer, proximal scansors have a lower estimated detachment angle (the angle of the scansor induced by digital hyperextension by which all setae are raised to 30° or any other given angle) than do the shorter distal scansors. This likely facilitates detachment because the digit is rolled off the surface from the distal end proximally. As a result of hyperextension, distal scansors are raised to a higher angle first, whereas proximal scansors are raised later and to a lesser extent (Russell, 2002: Fig. 3). Associated shorter setae are able to detach at a lower hyperextension angle (but an identical critical angle because the setae are absolutely shorter).

Setal density tends to decrease along the length of the scansor, which is related to the increasing diameter of the proximally located setae. These larger structures take up more room than the thinner, distal setae, and therefore their density is lower. However, while there are relatively fewer setae in the proximal region, these structures tend to have very large cumulative setal tip areas, much larger than those of the slender distal setae (Fig. 2D). As a result, overall tip density may not change greatly across the scansor, even though setal density does. Examination of

the setal tips of *Rhoptropus* revealed setal tip densities of 6.0×10^6–8.0×10^6, and 9.0×10^6–1.0×10^7 tips mm^{-2} for the distal/intermediate and proximal regions of the scansors, respectively, suggesting that the density of setal tips for the proximal region of a scansor may be higher that that of the distal or intermediate regions; however, further investigation of this trend is required before any firm conclusions can be drawn.

An exception to the trend of decreasing setal density along a scansor occurs at the proximal end of the proximal-most scansor. In this region setal density increases, which is likely the result of the decrease in diameter of the setal structures in this area, resulting in tighter packing of the structures. These trends in setal density are fairly constant between species, with similar densities observed at homologously similar locations between species across the entire adhesive apparatus. From this it is predicted that all species of *Rhoptropus* will have similar adhesive capabilities when normalized for pad area.

Interspecific variation and the case of *R. afer* – evolutionary, ecological and phylogenetic implications

Significant interspecific variation occurs for only a small proportion of the traits and species examined. For the most part, all of the species of the *Rhoptropus* radiation, as well as the outgroup taxon *C. bibronii*, exhibit setal field morphologies that are not significantly different from each other once they have been scaled for size. One notable exception is *R. afer.* The results of multiple conventional and phylogenetic statistical tests, including PCA, DFA, Moran's I and phylogenetically adjusted ANOVAs, all suggest that this species differs substantially from its congeners. *Rhoptropus afer* possesses significantly shorter setae (maximum, minimum and average length) than do most of the other species examined, and has significantly smaller subdigital pads relative to its size than do many of the other species. Results of the DFAs support this trend, with *R. afer* being able to be discriminated from its congeners based on setal length and pad area with a high percentage of success.

Significant differences were also found consistently for the pad area of *R.* cf. *biporosus*; however, this could be the result of the analysis of a variety of different digits, not just digit IV of the pes, for this species. If this is the case it is important to note that *R.* cf. *biporosus* and *R. biporosus* (the two species for which multiple different digits were analyzed) did not show differences in any other aspect of setal field morphology, suggesting that all digits are similar in overall setal field patterning, even though subdigital pad area may vary. It has been shown, however, that pad area does not tend to vary significantly between digits (Delannoy, 2006; Webster et al. 2009), and thus *R.* cf. *biporosus* may possess slightly smaller pads than some other species of *Rhoptropus.* Behavioral and ecological characteristics of this undescribed species are not yet known, making it difficult to explain this difference. The sister species of *R.* cf. *biporosus*, *R. biporosus*, has been noted to prefer horizontal surfaces more than do other species of *Rhoptropus* (with the exception of *R. afer*) (Branch, 1988; Bauer et al. 1996; Johnson et al. 2005), and perhaps this trend is continued in *R.* cf. *biporosus*, resulting in smaller subdigital pads in this species. There is, however, no evidence at this time to support this hypothesis.

Returning to a consideration of *R. afer*, this species is highly different from its congeners, and this is strongly linked to phylogeny (Fig. 6). This is not surprising, because the genetic distance between *R. afer* and its congeners is high when compared to the distances between other species, even though it has not been evolving for a much greater time period (Bauer, 1999). This asymmetry in the genetic distance measures suggests that the rate of evolution of *R. afer* has been faster than that for the other species in the genus, resulting in an increased rate of allozymic change as well as many differences in morphology (Bauer & Good, 1996; Bauer, 1999). However, despite the large phylogenetic effect detected for *R. afer*, the difference in setal length and pad area between it and other species remains significant even when these phylogenetic effects are taken into account. This implies that ecological factors have been driving the rapid evolution of this species.

The unique morphological and behavioral characteristics of *R. afer* at the whole body level are well documented. This species has features that have been purported to be adaptations for a more terrestrial and cursorial lifestyle. For example, it possesses significantly longer limb segments relative to those of other *Rhoptropus*, including its sister species *R. bradfieldi*, and all other members of the *Pachydactylus* radiation (Bauer et al. 1996; Johnson et al. 2005). These elongated components include all segments of the limb, pes and digits, with the exception of the ultimate and penultimate phalanges, which are constrained by their association with the scansorial apparatus (Bauer et al. 1996). *Rhoptropus* in general has a reduced number of presacral vertebrae, and exhibits secondary asymmetry of the pes, compared to other pad-bearing geckos, which possess nearly symmetrical feet, associated with even weight distribution while climbing (Russell & Bauer, 1989). These characteristics may be associated with the shift of all members of *Rhoptropus* from a rock crevice dwelling and a slow climbing lifestyle, common in *Pachydactylus* and *Chondrodactylus*, to a more active, running and jumping diurnal lifestyle. This shift reaches its extreme in *R. afer*, which is highly adapted for speed on flat surfaces (Bauer et al. 1996). The major differences found in *R. afer* appear to be autapomorphic, suggesting that they are not wholly reflections of the phylogenetic trends within the genus, and intimate that this species is highly divergent. Allozyme data indicate that this rapid divergence may have occurred as much as 9.6–15.6 MYA, and may be related to Miocene

geological and/or climatic changes associated with evolution of the Namib Desert (Bauer & Good, 1996; Bauer, 1999).

These differences in limb morphology are further exemplified here at the level of subdigital and setal field morphology of this species. The setal field configuration and geometry of other *Rhoptropus* species do not differ significantly from that of the outgroup *C. bibronii*, suggesting that these characteristics are primitive and have been conserved in the majority of the radiation. Although *Rhoptropus* tends to move more rapidly than do other members of the *Pachydactylus* radiation (such as *C. bibronii*), the majority of the included species are still climbers and spend most of their time moving on vertical or near-vertical rock faces (Odendaal, 1979; Haacke & Odendaal, 1981; Branch, 1988; Bauer et al. 1993). As such, these species disport a well-developed and functional adhesive system. Conversely, *R. afer* is much more terrestrial, moving largely on sand or other flat surfaces (Odendaal, 1979; Haacke & Odendaal, 1981; Branch, 1988; Bauer et al. 1993), and apparently is less dependent on its adhesive system. The results suggest that *R. afer* demonstrates some degree of subdigital pad reduction associated with its terrestrial lifestyle (Bauer et al. 1996; Russell et al. 1997), which is indicated here by its relatively smaller subdigital pads and lower scansor number. This pattern of pad reduction is reflected in setal length as well, with *R. afer* possessing shorter setae than its congeners. Other setal field characteristics, including general setal morphology and configuration patterns, setal diameter and setal density, are, however, conserved, suggesting that *R. afer* possesses a functional adhesive system. This species should, therefore, be capable of climbing locomotion on rock surfaces, which is consistent with observations that it will occupy boulders or rock faces in the absence of its congeners (Haacke & Odendaal, 1981).

The adaptive value of reduced subdigital pads and shortened setae for a more terrestrial lifestyle is uncertain. Smaller pads at the ends of elongated digits likely facilitate running on flat surfaces. While moving on flat surfaces, *Rhoptropus*, and other members of the *Pachydactylus* radiation, hold their subdigital pads in a hyperextended position, likely to prevent damage to or clogging of the setae by sandy or dusty substrates (Russell, 1975; Russell & Bauer, 1990). Although setae are self cleaning (Hansen & Autumn, 2005), constant exposure to dust and debris may limit the effectiveness of this property, especially on unconsolidated surfaces that may be less likely to accept donated particulate matter from the self-cleaning setae. Reducing the extent of the subdigital pads and elongating the remaining segments of the digit allows for a relatively much greater proportion of the subdigital area to be in contact with the surface during terrestrial locomotion, thereby allowing more thrust to be generated and resulting in faster, more effective cursorial locomotion (Bauer et al. 1996). Reduction in pad area could also facilitate detachment of the subdigital pads from the substrate. Smaller pads could be removed more rapidly, allowing faster locomotion across a surface. Reduction in relative pad size also suggests that the adhesive capabilities of *R. afer* are reduced, as it possesses fewer setae than do other *Rhoptropus* species of similar size. Thus, although it would be capable of climbing vertical surfaces, it may not be able to do so as effectively as its congeners.

Explaining the potential adaptive value of reduction in setal length is more difficult. The effect of reduced setal length on adhesive ability is unclear. Shorter setae would not be able to penetrate as deeply into uneven surfaces, which could reduce the number of setae able to contact the surface (especially on undulant substrata), thereby decreasing the amount of adhesive force able to be generated. However, setal length in *R. afer* may also relate to the types of surfaces on which it habitually moves/climbs. These surfaces have not yet been effectively sampled, making it difficult to draw conclusions about how their setae would interact with them. One potential benefit of reduced setal length is the facilitation of detachment. Shorter setae would reduce the estimated hyperextended detachment angle of the scansors for any given critical setal release angle. Together with the relatively small size of the pads, this would allow more rapid detachment of the subdigital pads, which may be beneficial to a fast-moving species like *R. afer*.

Rhoptropus afer is not the only species in the *Pachydactylus* radiation to demonstrate reduction of the subdigital pads. A rupicolus (rock-climbing) lifestyle is the primitive state for the clade; however, transitions to terrestriality have occurred at least eight times, with five of the eight terrestrial forms inhabiting sandy substrates (Lamb & Bauer, 2006). These species all demonstrate various levels of subdigital pad reduction. First, some species including *Pachydactylus austeni* Hewitt 1923 and *Colopus kochii* (Fitzsimons 1959), demonstrate very low counts of about two to three scansors, which is lower than the five to six seen in *R. afer*. Secondly, other taxa, including some *Colopus* and *Pachydactylus vanzyli* (Steyn & Haacke 1966), show extreme reduction of the subdigital apparatus. Finally, species such as *Pachydactylus rangei* (Andersson 1908) and *Chondrodactylus angulifer* are entirely padless (Lamb & Bauer, 2006). Therefore, subdigital pad reduction associated with a terrestrial lifestyle is a repeated theme in the *Pachydactylus* radiation. As setal field morphology has been shown to be fairly constrained and conserved among *Rhoptropus*, as well as in *C. bibronii*, it would be informative to examine the subdigital outgrowths of species showing a greater degree of pad reduction than does *R. afer*, to see whether the trend of decreasing setal length encountered there is present to a greater degree in these other species. Also, *R. afer* maintains an ordered arrangement of subdigital structures; however, during the loss of adhesive structures, this ordered arrangement may break down at some point,

with patterns becoming more random and unpredictable. For example, in *C. angulifer*, the distal part of the digit is highly reduced, and shows a highly modified pattern of skeletal elements in this region (Haacke, 1976). Examining gekkotan species exhibiting varying degrees of pad reduction may reveal a similar trend in loss of setal field organization with increasing levels of pad reduction. Determining if, and at what stage in pad loss, this transition occurs would be a key discovery in the study of the evolution of pad loss in geckos.

Concluding remarks

The configuration of setal fields among geckos appears to be fairly conserved and follows a similar and distinctive pattern between genera and species. This is observed in the species of *Rhoptropus* from southern Africa, in which setal field morphology and characteristics are ostensibly the same for all species, as well as for the outgroup species *C. bibronii.* Overall, a generalized *Rhoptropus* subdigital pad has the following six characteristics (Fig. 4): (1) Setal length decreases along the length of each scansor from the distal to the proximal end, with overall setal lengths also decreasing proximally from one scansor to the next. (2) Although setal length varies between scansors, the difference in length between the longest and shortest seta on each scansor remains constant, with average differential values for all species of 31–32 μm. (3) Setal diameter increases along the length of each scansor but does not change significantly between scansors. (4) Scansor length and the number of setal rows per scansor both increase proximally. (5) Setal density decreases along the length of each scansor, with the exception of the proximalmost scansor , where density increases at the proximal end. (6) The length and diameter of the setae influences their effective elastic moduli and bending stiffness, with long, thin, distally positioned setae having a very low effective elastic modulus and bending stiffness, and setae at the proximal end of the scansor having a much higher E_{eff} and bending stiffness.

One species in the genus, however, exhibits characteristics related to subdigital pad reduction associated with the adoption of more terrestrial lifestyle, but it maintains functional pads with the same basic pattern of organization seen in species showing no pad reduction. Relative pad size and setal length are reduced in this species, but setal diameter, density and pattern of arrangement remain unchanged.

Returning to our hypotheses, we predicted that setal dimensions would vary according to station on the digit and on any given scansor, and would vary in association with identifiable aspects of digital morphology. These predictions were borne out for all species examined and the pattern of variation is gradationally arranged along the pad and along individual scansors. The revealed pattern of length changes can be correlated with digital form and the process of digital hyperextension, and with the deployment of the setae as they are lowered onto, and raised from, the locomotor substratum. Setae are stratified in length in relation to how the integrated fields of setae operate: as a unified system capable of adjusting to local irregularities in the terrain. There is, therefore, no length of seta that is typical of a species and comparative reporting of setal lengths between species is only meaningful if anatomically equivalent regions of the digit are referred to. By comparing setal field dimensions it is possible to demonstrate that the setae of *R. afer* are shorter than those of other species of the genus at all stations along the pad, but randomly selected individual setae would not necessarily yield the same information.

We further predicted that within a radiation there would be common assembly rules for the setal fields, with variation being related to subdigital pad dimensions and numbers of scansors. Again this was borne out. All species of *Rhoptropus* have similarly configured setal fields, although the actual dimensions and constitution of the subdigital pad vary between species. This suggests that a common and integrated developmental pattern underlies the expression of the epidermal outgrowths that constitute the microfibrillar arrays. This is further borne out by developmental data available for the closely related *C. bibronii* (Webster et al. 2009) which exhibits incremental changes to setal field dimensions and absolute setal lengths as growth occurs from hatching to adult.

These findings have implications for how the setal fields of *Rhoptropus* are configured in relation to the natural substrates upon which each species moves (which is the subject of a separate contribution), and for the design principles used for generating and manufacturing artificial microfibrillar arrays intended to reproduce the adhesive capabilities of gekkotan setae. Considering how the entire set of microfibrillar outgrowths is configured in geckos may provide insights into the structuring of artificial arrays intended to be employed in dynamic situations in which some facsimile of digital hyperextension is used to lower the microfibrils toward the surface to make contact, and to remove them from contact, as progression occurs.

Acknowledgements

We thank Heather Jamniczky, Aaron M. Bauer and the field party in Namibia who helped with the collection of material used in this research. We thank Jim Hanken and José Rosado, Museum of Comparative Zoology, Harvard University, for the loan of study specimens. The comments of two anonymous reviewers were of great assistance in helping us to clarify concepts and arguments. An NSERC Discovery grant to A.P.R., an NSERC studentship grant, and an Alberta Ingenuity Fund grant to M.K.J. supported this research. SEM work was done at the University of Calgary Microscopy and Imaging Facility.

References

Albrecht GH, Gelvin BR, Hartman SE (1993) Ratios as a size adjustment in morphometrics. *Am J Phys Anthropol* **91**, 441–468.

Altevogt R (1954) Probleme eines Fusses. *Kosmos Stuttgart* **9**, 428–430.

Andersson LG (1908) A remarkable new gecko from South Africa and a new *Stenocercus* species from South America in the Natural History Museum in Wiesbaden. *Nassau Ver F Naturk Wiesbaden* **61**, 299–306.

Arzt E, Gorb S, Spolenak R (2003) From micro to nano contacts in biological attachment devices. *Proc Natl Acad Sci USA* **100**, 10603–10606.

Autumn K (2006) Properties, principles, and parameters of the gecko adhesive system. In *Biological Adhesives* (eds Smith AM, Calow JA), pp. 225–256. Berlin: Springer-Verlag..

Autumn K, Peattie AM (2002) Mechanisms of adhesion in geckos. *Integr Comp Biol* **42**, 1018–1090.

Autumn K, Liang YA, Hsleh ST, et al. (2000) Adhesive force of a single gecko foot-hair. *Nature* **405**, 681–685.

Autumn K, Sitti M, Liang YA, et al. (2002) Evidence for van der Waals adhesion in gecko setae. *Proc Natl Acad Sci USA* **99**, 12252–12256.

Autumn K, Dittmore A, Santos D, Spenko M, Cutkosky M (2006a) Frictional adhesion: a new angle on gecko attachment. *J Exp Biol* **209**, 3569–3579.

Autumn K, Majidi C, Groff RE, Dittmore A, Fearing R (2006b) Effective elastic modulus of isolated gecko setal arrays. *J Exp Biol* **209**, 3558–3568.

Bauer AM (1999) Evolutionary scenarios in the *Pachydactylus* group geckos of southern Africa: new hypotheses. *Afr J Herpetol* **48**, 53–62.

Bauer AM, Good DA (1996) Phylogenetic systematics of the day geckos, genus *Rhoptropus* (Reptilia: Gekkonidae), of south-western Africa. *J Zool Lond* **238**, 635–663.

Bauer AM, Lamb T (2002) Phylogenetic relationships among members of the *Pachydactylus capensis* group of southern African geckos. *Afr Zool* **37**, 209–220.

Bauer AM, Lamb T (2005) Phylogenetic relationships of southern African geckos in the *Pachydactylus* group (Squamata: Gekkonidae). *Afr J Herpetol* **54**, 105–129.

Bauer AM, Branch WR, Haacke WD (1993) The herpetofauna of the Kamanjab area and adjacent Damaraland, Namibia. *Madoqua* **18**, 117–145.

Bauer AM, Russell AP, Powell GL (1996) The evolution of locomotor morphology in *Rhoptropus* (Squamata: Gekkonidae): functional and phylogenetic considerations. *Afr J Herpetol* **45**, 8–30.

Bowden FP, Tabor D (1966) Friction, lubrication and wear: a survey of work during the last decade. *Br J Appl Phys* **17**, 1521–1544.

Branch B (1988) *Field Guide to the Snakes and other Reptiles of Southern Africa*. Cape Town: Struik Publishers.

Brown RM, Alcala AC (2000) Geckos, cave frogs, and small landbridge islands in the Visayan sea. *Haring Ibon* **2**, 19–22.

Brown RM, McGuire JA, Ferner W, Icarangal N Jr, Kennedy RS (2000) Amphibians and reptiles of Luzon Island, II: Preliminary report on the herpetofauna of Aurora National Park, Philippines. *Hamadryad* **25**, 175–195.

Brown WC, Alcala AC (1978) *Philippine Lizards of the Family Gekkonidae*. Dumaguete City, Philippines: Silliman University Press.

Campolo D, Jones S, Fearing R (2003) Fabrication of gecko foot-hair like nano structures and adhesion to random rough surfaces. *Nanotechnology* **2**, 856–859.

Cliff AD, Ord JK (1973) *Spatial Autocorrelation*. London: Pion.

Cliff AD, Ord JK (1981) *Spatial Processes: Models and Applications*. London: Pion.

Cocozzelli C (1988) Understanding canonical discriminant function analysis testing typological hypotheses. *J Soc Serv Res* **11**, 93–117.

Collette BB (1961) Correlations between ecology and morphology in anoline lizards from Havana, Cuba and southern Florida. *Bull Mus Comp Biol* **125**, 137–162.

Delannoy S (2006) *Subdigital setae of the Tokay gecko (*Gekko gecko*): Variation in form and implications for adhesion* MSc, University of Calgary.

Dellit WF (1934) Zur Anatomie und Physiologie der Geckozehe. *Jena Z Naturwiss* **68**, 613–656.

Dellit WF (1949) Zum Haftproblem der Geckoniden. *Dtsch Aquar Terr Z* **2**, 56–58.

Epperson BK, Chung MG (2001) Spatial genetic structure of allozyme polymorphisms within populations of *Pinus strobus* (Pinaceae). *Am J Bot* **88**, 1006–1010.

Felsenstein J (1985) Phylogenies and the comparative method. *Am Nat* **125**, 1–15.

FitzSimons V (1957) Reptilia. Serpentes and Sauria. In *South African Animal Life Results of the Lund University Expedition in 1950–1951* (eds Hanström-Perbrinck B, Rudebeck G), pp. 385–405 Stockholm: Almqvist and Wiksell.

FitzSimons V (1959) Some new reptiles from southern Africa and southern Angola. *Ann Transvaal Mus* **23**, 405–409.

Gadow H (1901) Amphibia and Reptiles. In *The Cambridge Natural History* (eds Harmer SF, Shipley AC), pp. xiii + 1–668. London: Macmillan and Co. Ltd.

Garland TJ, Harvey PH, Ives IR (1992) Procedures for the analysis of comparative data using phylogenetically independent contrasts. *Syst Zool* **41**, 18–32.

Garland TJ, Dickerman AW, Janis CM, Jones JA (1993) Phylogenetic analysis of covariance by computer simulation. *Syst Biol* **42**, 265–292.

Geim AK, Dubonos SV, Grigorieva IV, Novoselov KS, Zhukov AA (2003) Microfabricated adhesive mimicking gecko foot-hair. *Nat Mater* **2**, 461–463.

Gittleman JL, Kot M (1990) Adaptation: statistics and a null model for estimating phylogenetic effects. *Syst Zool* **39**, 227–241.

Glassmaker NJ, Jagota A, Hui CY, Kim J (2004) Design of biomimetic fibrillar interfaces: 1, Making contact. *J R Soc Interface* (doi:10.1098/rsif.2004.0004).

Günther A (1864) *The Reptiles of British India*. London: The Ray Society, pp. xxvii, 452, 26 plates.

Guo C, Wang W, Yu M, Dai Z, Sun J (2007) Comparative studies on the structure and adhesion of setae in *G. gecko* and *G. swinhonis*. *Sci China Ser C* **50**: 831–838.

Haacke WD (1965) Additional notes on the herpetology of South West Africa with descriptions of two new subspecies of geckos. *Cimbebasia* **11**, 1–39.

Haacke WD (1976) Burrowing geckos of Southern Africa, 2 (Reptilia: Gekkonidae). *Ann Transvaal Mus* **30**, 13–28, plate 1.

Haacke WD, Odendaal FJ (1981) The distribution of the genus *Rhoptropus* (Reptilia: Gekkonidae) in the central Namib Desert. *Madoqua* **12**, 199–215.

Hansen WR, Autumn K (2005) Evidence for self-cleaning in gecko setae. *Proc Natl Acad Sci USA* **102**, 385–389.

Harvey PH, Pagel MD (1991) *The Comparative Method in Evolutionary Biology*. Oxford: Oxford University Press.

Hecht MK (1952) Natural selection in the lizard genus. *Aristelliger. Evolution* **6**, 112–124.

Hewitt J (1923) Descriptions of two new S. African geckos of the genus *Pachydactylus. Ann Natal Mus* **5**, 67–71.

Hewitt J (1926) Descriptions of new and little known lizards and batrachians from South Africa. *Ann South African Mus (Cape Town)* **20**, 413–431.

Hewitt J (1935) Some new forms of batrachians and reptiles from South Africa. *Rec Albany Mus* **4**, 283–357.

Hiller U (1968) Untersuchungen zum Feinbau und zur Funktion der Haftborsten von Reptilien. *Morph Tiere* **62**, 307–362.

Hiller U (1969) Correlation between corona-discharge of polyethylene films and the adhering power of *Tarentola m. mauritanica* (Rept.). *Forma et Functio* **1**, 350–352.

Hiller U (1976) Comparative studies on the functional morphology of two gekkonid lizards. *J Bombay Nat Hist Soc* **73**, 278–282.

Hora SL (1923) The adhesive apparatus on the toes of certain geckos and tree frogs. *J Proc Asiatic Soc Bengal* **19**, 138–145.

Huber G, Mantz H, Spolenak R, et al. (2005) Evidence for capillarity contributions to gecko adhesion from single spatula nanomechanical measurements. *Proc Natl Acad Sci U S A* **102**, 16293–16296.

Hui CY, Glassmaker NJ, Tang T, Jagota A (2004) Design of biomimetic fibrillar interfaces: 2. Mechanics of enhanced adhesion. *J R Soc Interface* (doi10.1098/rsif.2004.005).

Jagota A, Bennison SJ (2002) Mechanics of adhesion through a fibrillar microstructure. *Integr Comp Biol* **42**, 1140–1145.

Johnson MK, Russell AP, Bauer AM (2005) Locomotor morphometry of the *Pachydactylus* radiation of lizards (Gekkota: Gekkonidae): a phylogenetically and ecologically informed analysis. *Can J Zool* **83**, 1511–1524.

Kaiser HF (1958) The varimax criterion for analytic rotation in factor analysis. *Psychometrika* **23**, 187–200.

Karlis D, Sapporta G, Spinakis A (2003) A simple rule for the selection of principal components. *Commun Stat A-Theor* **32**, 643–666.

Kim S, Spenko M, Trujillo S, Heynemen B, Mattoli V, Cutkosky MR (2007) Whole body adhesion: hierarchical, directional and distributed control of adhesive forces for a climbing robot, *IEEE Int Conf Robotics Autom* April, **10–14**, 1268–1273.

Kunitzky J (1903) Die Zeit der Entstehung der Borsten und Mechanismus der Bewegung bei den Geckotiden (*Ptychozoon homalochephalim* Crev). *Bull Acad Imper Sci St Petersbourg* **18**, 21–24.

Kustandi TS, Samper VD, Ng WS, Chong AS, Gao H (2007) Fabrication of a gecko like hierarchical fibril array using a bonded porous alumina template. *J Micromech Microeng* **17**, N75–N81.

Lamb T, Bauer AM (2000) Relationships of the *Pachydactylus rugosus* group of geckos (Reptilia: Squamata: Gekkonidae). *Afr Zool* **35**, 55–67.

Lamb T, Bauer AM (2001) Mitochondrial phylogeny of Namib Day Geckos (*Rhoptropus*) based on cytochrome b and 16S rRNA sequences. *Copeia* **2001**, 775–780.

Lamb T, Bauer AM (2002) Phylogenetic relationships of the large-bodied members of the African lizard genus *Pachydactylus* (Reptilia: Gekkonidae). *Copeia* **2002**, 586–596.

Lamb T, Bauer AM (2006) Footprints in the sand: independent reduction of subdigital lamellae in the Namib–Kalahari burrowing geckos. *Proc R Soc Lond B* **273**, 855–864.

Laurent RF (1964) Reptiles et batraciens de l'Angola (troisième note). *Companhia de Diamantes de Angola (Diamang), Serviços Culturais, Museu do Dundo (Angola)* **67**, 165.

Lee J, Majidi C, Schubert B, Fearing R (2008) Sliding-induced adhesion of stiff polymer microfibre arrays. I. Macroscale behaviour. *J R Soc Interface* doi:10.1098/rsif.2007.1308, published online.

Linnaeus C (1758) *Systema naturæ per regna tria naturæ, secundum classes, ordines genera, species, cum characteribus, differentiis, synonymis, locis* Tomus I. Editio decima, reformata. Laurentii Salvii, Holmiæ. 10th edn, 824 pp.

Maderson PFA (1964) Keratinized epidermal derivatives as an aid to climbing in gekkonid lizards. *Nature* **203**, 780–781.

Maderson PFA (1970) Lizard hands and lizard glands: Models for evolutionary study. *Forma Functio* **3**, 179–204.

Mahendra BC (1941) Contributions to the bionomics, anatomy, reproduction and development of the Indian house gecko *Hemidactylus flaviviridis* Rüppel, Part II: The problem of locomotion. *Proc Ind Acad Sci B* **13**, 288–306.

Martins EP, Garland TJ (1991) Phylogenetic analyses of the correlated evolution of continuous characters: a simulation study. *Evolution* **45**, 534–547.

Meine K, Kloß K, Schneider T, Spaltman D (2004) The influence of surface roughness on the adhesion force. *Surf Interface Anal* **36**, 694–697.

Moran PAP (1950) Notes on continuous stochastic phenomena. *Biometrika* **37**, 17–23.

Nei M (1978) Estimation of average heterozygosity and genetoc distance from a small number of individuals. *Genetics* **89**, 583–590.

Odendaal FJ (1979) Notes on the adaptive ecology and behaviour of four species of *Rhoptropus* (Gekkonidae) from the Namib Desert with special reference to a thermoregulatory mechanism employed by *Rhoptropus afer*. *Madoqua* **11**, 255–260.

Peressadko A, Gorb S (2004) When less is more: Experimental evidence for tenacity enhancement by division of contact area. *J Adhesion* **80**, 247–261.

Persson BNJ (2003) On the mechanism of adhesion in biological systems. *J Chem Phys* **118**, 7614–7621.

Persson BNJ, Gorb S (2003) The effect of surface roughness on the adhesion of elastic plates with application to biological systems. *J Chem Phys* **119**, 11434–11437.

Peters WCH (1869) Eine Mittheilung über neue Gattungen und Arten von Eidechsen. Berlin: Monatsber. Königl Preuss Akad Wissensch. **1869**: 57–66.

Peterson JA (1983) The evolution of the subdigital pad of *Anolis.* 2. Comparisons among iguanid genera related to the anolines and a view from outside the radiation. *J Herpetol* **17**, 371–397.

Peterson JA, Williams EE (1981) A Case history in retrograde evolution: the *Onca* lineage in anoline lizards. II. Subdigital fine structure. *Bull Mus Comp Biol* **149**, 215–268.

Peterson JAJ, Benson A, Ngai M, Morin J, Ow C (1982) Scaling in tensile 'skeletons': structures with scalo-independent length dimensions. *Science* **217**, 1267–1270.

Pimentel RA (1979) *Morphometrics: The Multivariate Analysis of Biological Data*. Dubuque, IA: Kendall/Hunt Publishing Co.

Roesler H, Siler CD, Brown RM, Demegillo AD, Gaulke M (2006) *Gekko ernstkelleri* sp. n. – a new gekkonid lizard from Panay Island, Philippines. *Salamandra* **42**, 197–211.

Ruibal R, Ernst V (1965) The structure of the digital setae of lizards. *J Morphol* **117**, 271–294.

Russell AP (1972) *The foot of gekkonid lizards: a study in comparative and functional anatomy*. PhD Thesis. University of London.

Russell AP (1975) A contribution to the functional analysis of the foot of the Tokay, *Gekko gecko* (Reptilia: Gekkonidae). *J Zool Lond* **176**, 437–476.

Russell AP (1976) Some comments concerning interrelationships amongst gekkonine geckos. In *Morphol Biol Reptiles Linnean Soc Symposium Series 3* (eds Bellairs AdA, Cox CB), pp. 217–244. London: Academic Press.

Russell AP (1986) The morphological basis of weight-bearing in the scansors of the tokay gecko (*Gekko gecko*). *Can J Zool* **64**, 948–955.

Russell AP (2002) Integrative functional morphology of the gekkotan adhesive system (Reptilia: Gekkota). *Integr Comp Biol* **42**, 1154–1163.

Russell AP, Bauer AM (1986) Le gécko géant *Hoplodactylus delcourti* et ses relations avec le gigantisme et l'endemisme insulaire chez les Gekkonidae. *Mesogée Marseille* **46**, 25–28.

Russell AP, Bauer AM (1989) The morphology of the digits of the golden gecko, *Calodactylodes aureus* and its implications for the occupation of rupicolous habitats. *Amphibia-Reptilia* **10**, 125–140.

Russell AP, Bauer AM (1990) Hypertrophied phalangeal chondroepiphyses in the gekkonid genus *Phelsuma*: their structure and relation to the adhesive mechanism. *J Zool Lond* **221**, 205–217.

Russell AP, Johnson MK (2007) Real world challenges to, and capabilities of, the gekkotan adhesive system: contrasting the rough and the smooth. *Can J Zool* **85**, 1228–1238.

Russell AP, Bauer AM, Laroiya R (1997) Morphological correlates of the secondarily symmetrical pes of gekkotan lizards. *J Zool Lond* **241**, 767–790.

Russell AP, Johnson MK, Delannoy SM (2007) Insights from studies of gecko-inspired adhesion and their impact on our understanding of the evolution of the gekkotan adhesive system. *J Adhesion Sci Technol* **21**, 1119–1143.

Schleich H, Kästle W (1986) Ultrastrukturen an Gecko-Zehen (Reptilia: Sauria: Gekkonidae). *Amphibia-Reptilia* **7**, 141–166.

Schmidt H (1905) Zur Anatomie und Physiologie der Geckopfote. *Jena Z Naturwiss* **39**, 551–580 + plate 1.

Schultz BB (1985) Levene's test for relative variation. *Syst Zool* **34**, 449–456.

Silvertown J, Dodd M (1996) Comparing plants and connecting traits. *Philos Trans R Soc B* **351**, 1233–1239.

Simmermacher VG (1884) Hafftapparate bei Wirbeltieren. *Zool Garten* **25**, 289–301.

Sitti M, Fearing R (2003) Synthetic gecko foot-hair micro/nanostructures as dry adhesives. *J Adhes Sci Technol* **17**, 1055–1073.

Smith A (1846) *Illustrations of the Zoology of South Africa, Reptilia*. London: Smith, Elder, and Co.

Spolenak R, Gorb S, Gao H, Artz E (2004) Effects of contact shape on the scaling of biological attachments. *Proc R Soc Lond A* **2004**, 1–15.

Spolenak R, Gorb S, Arzt E (2005) Adhesion design maps for bio-inspired attachment systems. *Acta Biomater* **1**, 5–13.

Stewart GR, Daniel RS (1972) Scales of the lizard *Gekko gecko*: surface structure examined with the scanning electron microscope. *Copeia* 1**972**, 252–257.

Steyn W, Haacke WD (1966) A new webfooted gekko (*Kaokogecko vanzyli* gen. et. sp. nov.) from the north-western South West Africa. *Cimbebasia* **18**, 1–3.

Stork NE (1983) A comparison of the adhesive setae on the feet of lizards and arthropods. *J Nat Hist* **17**, 829–835.

Sun W, Neuzil P, Kustandi TS, Oh S, Samper VD (2005) The nature of the gecko lizard adhesive force. *Biophys J Biophys Lett* **89**, L14–L17.

Tandler J (1903) Beiträge zur Anatomie der Geckopfote. *Z Wissenschaft Zool* **75**, 308–326.

Tian Y, Pesika N, Zeng H, et al. (2006) Adhesion and friction in gecko toe attachment and detachment. *Proc Natl Acad Sci USA* **103**, 19320–19325.

Tornier G (1899) Ein Eidechsenschwanz mit Saugscheibe. *Biol Centralblatt* **19**, 549–552.

Vogel S (2003) *Comparative Biomechanics*. Princeton: Princeton University Press.

Webster NB, Johnson MK, Russell AP (2009) Ontogenetic scaling of scansorial surface area and setal dimensions of *Chondrodactylus bibronii* (Gekkota: Gekkonidae): testing predictions derived from cross-species comparisons of gekkotans. *Acta Zool* **90**: 18–29.

Weitlaner F (1902) Eine Untersuchung über den Haftfuss des Gecko. *Verhandlung Zool Bot Ges Wein* **52**, 328–332.

Wilkinson L (2007) *SYSTAT*. Chicago: SYSTAT Inc.

Supporting Information

Additional Supporting Information may be found in the online version of this article:

Table S1 Specimen numbers, collection information and digits removed

Table S2 Paired *t*-test results for each species examining the significance of differences between various measurements. (a) Maximum and minimum setal length on each scansor (distal, intermediate and proximal). (b) Maximum and minimum setal diameter on each scansor (distal, intermediate and proximal). (c) Mean setal length between scansors. (d) Mean setal diameter between scansors. (e) Mean setal density between scansors. Comparisons are significant if $P < 0.0033$ (Bonferroni adjusted value); these are marked with an asterisk.

Table S3 Component loadings for informative principal components (PCs) from three varimax-rotated principal component analyses. (a) Loadings from PCA I of distal scansor measurements. (b) Loadings from PCA II of intermediate scansor measurements. (c) PCA III of proximal scansor measurements. All measurements are log-transformed and measurements in each table (a,b,c) relate only to the associated scansor (a, distal; b, intermediate; c, proximal) with densities relating to the proximal, intermediate and distal regions of each scansor.

Please note: Wiley-Blackwell are not responsible for the content or functionality of any supporting materials supplied by the authors. Any queries (other than missing material) should be directed to the corresponding author for the article.